A Harmonic-Based Triple Phase Shift Modulation Strategy for a Dual Active Bridge Converter in an All Electric Aircraft Application

Bossi, Giuseppe; Song, Chaochao; Sangwongwanich, Ariya; Blaabjerg, Frede; Damiano, Alfonso

Published in:
2024 International Symposium on Power Electronics, Electrical Drives, Automation and Motion (SPEEDAM)

DOI (link to publication from Publisher):
10.1109/SPEEDAM61530.2024.10609059

Publication date:
2024

Document Version
Accepted author manuscript, peer reviewed version

A Harmonic-Based Triple Phase Shift Modulation Strategy for a Dual Active Bridge Converter in an All Electric Aircraft Application

Giuseppe Bossi
Dept. of Electric and Electronic Eng.
University of Cagliari
Cagliari, Italy
giuseppe.bossi@unica.it

Chaochao Song
AAU Energy
Aalborg University
Aalborg, Denmark
chso@energy.aau.dk

Ariya Sangwongwanich
AAU Energy
Aalborg University
Aalborg, Denmark
ars@energy.aau.dk

Frede Blaabjerg
AAU Energy
Aalborg University
Aalborg, Denmark
fbl@energy.aau.dk

Alfonso Damiano
Dept. of Electric and Electronic Eng.
University of Cagliari
Cagliari, Italy
damiano@unica.it

***Abstract*—A harmonic-based Triple-Phase Shift (TPS) modulation strategy for a 2.1kW, 270V Bidirectional DC-DC Dual Active Bridge (DAB) conditioning system for an All Electric Aircraft application is proposed in this paper. The DAB model has been obtained concerning the frequency domain, particularly resorting to the Fundamental Component Analysis (FCA). The TPS parameters are selected to both erase the flow-back current in the DC-link capacitor and minimize the voltage harmonic content on the load side. In this way, the reactive power minimization and the active power maximization associated with the first harmonic component are achieved. The co-simulation study of the proposed TPS shows a very good performances, also during step-load variations.**

***Index Terms*—DC/DC converters, dual active bridge, triple phase shift, harmonic analysis, all electric aircraft.**

I. Introduction

The All-Electric Aircraft (AEA) technology achieves the complete removal of the greenhouse-gasses emission during flight. This is possible because it avoids the use of fossil fuels as the energy source and, for this reason, is considered one of the most promising solutions for a less polluting aircraft design. In fact, the adoption of suitable Energy Storage Systems (ESS) and electric propellers allow for the exclusive use of electricity for developing all the activities associated with both propulsion and auxiliary avionic services [1].

In order to ensure the energy and power requirements in the AEA, suitable energy conversion systems are needed, which provide compliance with both the reliability and safety standards in all the operative conditions. For this reason, high-performance device solutions as Triple Active Bridge-based topologies are proposed in the literature, which provides the possibility to feed both the propulsion and auxiliary systems with one-high-efficiency device [2], [3].

This work has been developed within the framework of the project e.INS- Ecosystem of Innovation for Next Generation Sardinia (cod. ECS 00000038) funded by the Italian Ministry for Research and Education (MUR) under the National Recovery and Resilience Plan (NRRP) - MISSION 4 COMPONENT 2, "From research to business" INVESTMENT 1.5, "Creation and strengthening of Ecosystems of innovation" and construction of "Territorial R&D Leaders".

In these systems, the Single-Phase Shift (SPS) modulation strategy is applied, in which the power flow depends on the phase displacement between the primary and secondary sides 50% duty cycle voltage waveforms of the converter. This control strategy is simple and allows for achieving high power rates. Nevertheless, transformer core losses are present due to the non-sinusoidal magnetizing current waveform, and increase as much as output power is required [4]. Moreover, high flow-back currents in the DC-links are present in the SPS, which constitutes a reactive power component [5]. They lead to an higher amount of current transiting in the transformer and, besides higher power losses, it takes to a lower power rating utilization of the converter. Furthermore, it makes shorter the DC-link capacitors lifetime [6].

To overcome these issues, Double-Phase (DPS) and Triple-Phase Shift (TPS) control strategies are proposed in the literature [4]–[7]. Compared to SPS, DPS and TPS allow for changing the voltage duty cycle of the primary and secondary side at either same or different value, respectively. These modulation strategies add one or two more degree of freedom to the basic SPS control strategy. In this way, optimized current stresses on the components can be achieved, as well as an extended Zero-Voltage Switching (ZVS) operating area [8], [9]. Besides, other solutions are proposed in the literature to achieve these goals, as the employment of Neutral-Point Clamped (NPC) bridge topology instead of the H-bridge one, in which multi-level voltage waveforms allow adding further degree of freedom for optimizing the system [10], [11].

Many woks in the literature relies on the time-domain modelling of the converter, achieving high accuracy in forecasting its behaviour. However, they presents a very complex model with piece-wise equations, making difficult to manage all the possible converter working modes, especially when TPS control strategy is employed [12]–[14]. More simple yet accurate modelling that rely on the frequency domain are proposed, which resort on Fourier expansion analysis of the converter voltage waveforms. In particular, the Fundamental Component Analysis (FCA), which modelling relies on the

voltage first harmonic component, represents a very simple yet accurate analysis approach. The first harmonic component is responsible for almost entirely the active power content of the converter [15]–[17].

In this work, the FCA modelling approach applied on a Dual Active Bridge (DAB) converter is proposed. In particular, it relies on the phasorial notation and a graphical analysis of the converter behaviour. Moreover, a TPS control strategy is developed, which achieves both the harmonic minimization and the flow-back current cancellation on the converter output side. Finally, a co-simulation study has been carried out on PLECS and Matlab/Simulink considering a real laboratory DAB prototype model.

The paper is organized as follows: in Section II the DAB FCA analysis is developed; in Section III the TPS control strategy is elaborated; in Section IV the DAB model simulation results are presented and finally, in Section V the conclusion remarks are outlined.

II. Dual Active Bridge Model

The DAB is a bidirectional DC-DC converter that can work both in buck and boost modes, and its topology is reported in Fig. 1. It is composed of two full bridges FB^{in} and FB^{out} equipped with the DC-link capacitor banks C_i and C_o, respectively. Across the capacitors, the DC input and output voltages u^{in}_{DC} and u^{out}_{DC} are established. A magnetic tank is placed between the full bridges, and is composed of an High Frequency Transformer (HFT) and an external leakage inductance L_s. Particularly, the latter represents the key component for controlling the power generated in the converter. The main control strategy consists in generating two square-wave voltages u^{in}_{AC} and u^{out}_{AC} that, conveniently shifted across the leakage inductor, cause the current i^{in}_{AC} (i^{in}_{DC}) and i^{out}_{AC} (i^{out}_{DC}) to flow. This is called Single Phase Shift (SPS) modulation.

Nevertheless, in order to reduce the losses e.g. minimizing the circulating current and extending the soft-switching range, more sophisticated modulation strategies needs to be employed. Among various types, the Triple Phase Shift (TPS) represents one of the best solutions, in which the phase displacement between the legs of the full bridges are controlled separately, adding two more degree of freedom for controlling the converter [18], [19].

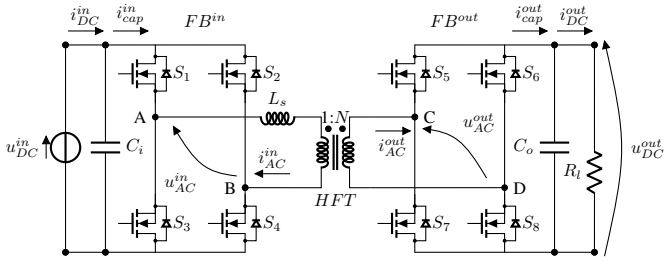

Fig. 1: Dual Active Bridge topology.

A. Frequency-Domain Model

The TPS square-wave voltages u^{in}_{AC} and u^{out}_{AC} are shown in Fig. 2. The duty cycles of the voltage waves change independently in the TPS, modifying their shape from a two-level to a three-level waveform. In particular, D_1 and D_2 represent the p.u duty cycles of the input and output voltages, respectively, while D_0 stands for their p.u. phase shift. All the three parameters are normalized over half period, and varies in accordance to (1)

$$\begin{cases} -0.5 \leq D_0 \leq 0.5 \\ 0 \leq D_1 \leq 1 \\ 0 \leq D_2 \leq 1. \end{cases} \tag{1}$$

The frequency-domain model is evaluated resorting to the Fourier series expansion, and its evolution is reported in (2) and (3) for both input and output voltages

$$u^{in}_{AC} = \frac{4}{\pi} u^{in}_{DC} \sum_{n=0}^{+\infty} \frac{\sin(nD_1\frac{\pi}{2})\cos(n\omega t)}{n} \tag{2}$$

$$u^{out}_{AC} = \frac{4}{\pi} u^{in}_{DC}\ k \sum_{n=0}^{+\infty} \frac{\sin(nD_2\frac{\pi}{2})\cos(n(\omega t - D_0\pi))}{n} \tag{3}$$

where $n = 1, 3, 5...$ is the harmonic order, ω is the angular frequency of the voltages, t is the time and

$$k = \frac{u^{out}_{DC}}{N u^{in}_{DC}}$$

is the voltage gain of the DAB, where N is the transformer turn ratio.

The first harmonic component phasors of both voltages are obtained for $n = 1$, $t = 0$, and are reported in (4) and (5).

$$\vec{u^{in}_{AC,1}} = \frac{4}{\pi} u^{in}_{DC} \sin\left(D_1\frac{\pi}{2}\right) \tag{4}$$

$$\vec{u^{out}_{AC,1}} = \frac{4}{\pi} u^{in}_{DC}\ k \sin\left(D_2\frac{\pi}{2}\right) e^{j(D_0\pi)} \tag{5}$$

Considering a clockwise rotation of the phasors allows for giving a positive phase-shift D_0 value, simplifying the model

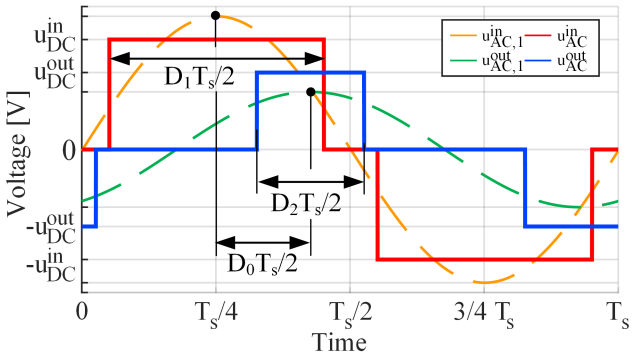

Fig. 2: Magnetic tank square voltage waveforms and their first harmonic component in TPS.

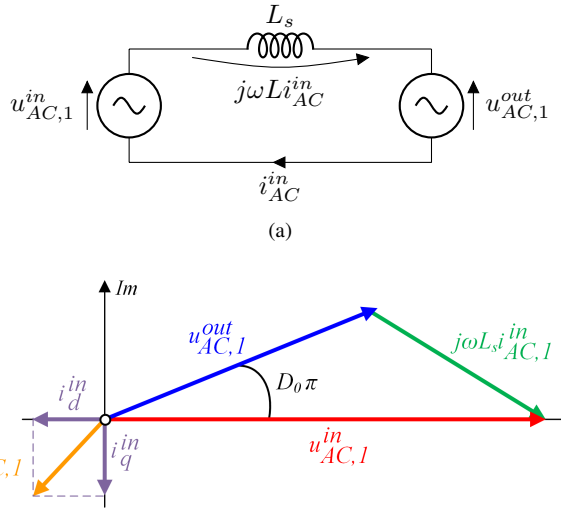

Fig. 3: a) DAB equivalent model concerning the first harmonic components b) Phasorial representation of voltage and current in the proposed TPS.

assessment. Moreover, it can be noted that the input and output voltage phasor length depends on D_1 and D_2, respectively, as it is in the voltage waves depicted in Fig. 2.

Referring to the DAB equivalent model reported in Fig. 3a, the current across the leakage inductance can be determined as (6)

$$\vec{i^{in}_{AC,1}} = \frac{\vec{u^{in}_{AC,1}} - \vec{u^{out}_{AC,1}}}{j\omega L_s}, \tag{6}$$

which graphical representation is reported in Fig. 3b.

Replacing (4) and (5) in (6), it assumes the final expression of (7)

$$\vec{i^{in}_{AC,1}} = \frac{4}{\pi\omega L_s} u^{in}_{DC} \cdot \cdot \left[k \sin\left(D_2 \frac{\pi}{2}\right) e^{j(D_0\pi + \frac{\pi}{2})} - j \sin\left(D_1 \frac{\pi}{2}\right) \right]. \tag{7}$$

By projecting the current phasor on the real and imaginary axis, the direct i^{in}_d and quadrature i^{in}_q current components are determined and reported in (8) and (9)

$$\vec{i^{in}_d} = \frac{4}{\pi\omega L_s} u^{in}_{DC} k \sin\left(D_2 \frac{\pi}{2}\right) \cos(D_0\pi + \frac{\pi}{2}) \tag{8}$$

$$\vec{i^{in}_q} = j\frac{4}{\pi\omega L_s} u^{in}_{DC} \cdot \cdot \left[k \sin\left(D_2 \frac{\pi}{2}\right) \sin\left(D_0\pi + \frac{\pi}{2}\right) - \sin\left(D_1 \frac{\pi}{2}\right) \right]. \tag{9}$$

Finally, the active and reactive power P and Q are obtained in (10) and (11) concerning (8) and (9), respectively, and the input voltage (4)

$$P = \frac{8}{\pi^2\omega L_s} u^{in^2}_{DC} \cdot \cdot k \sin\left(D_1 \frac{\pi}{2}\right) \sin\left(D_2 \frac{\pi}{2}\right) \cos\left(D_0\pi + \frac{\pi}{2}\right) \tag{10}$$

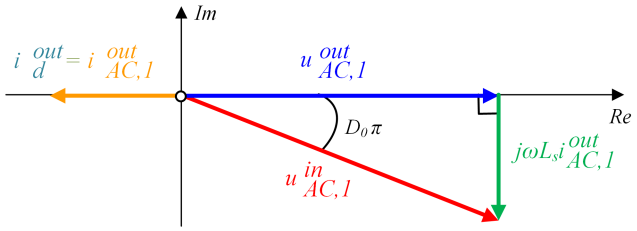

Fig. 4: Phasorial representation of voltage and current for output flow-back current elimination in the TPS.

$$Q = \frac{8}{\pi^2\omega L_s} u^{in^2}_{DC} \sin\left(D_1 \frac{\pi}{2}\right) \cdot \cdot \left[\sin\left(D_1 \frac{\pi}{2}\right) - k \sin\left(D_2 \frac{\pi}{2}\right) \sin\left(D_0\pi + \frac{\pi}{2}\right) \right]. \tag{11}$$

III. Triple Phase Shift Modulation

In this work, a TPS modulation strategy is proposed for achieving both the flow-back current cancellation in the DC-link and voltage harmonic content minimization at the output side. To achieve these targets, proper constraints to the DAB model needs to be applied, which are determined in the following.

A. Flow-back Current Cancellation

The flow-back current in the DC-link capacitor is responsible for the reactive power content in the converter i.e. its efficiency deterioration, and needs to be minimized [5]. Willing to completely erase the reactive current concerning the output side, the i^{out}_q component should be equal to zero, that is, the inductor current phase should be the same as the output voltage $u^{out}_{AC,1}$ one, and this condition is graphically represented in Fig. 4. It can be noted that, for simplifying the analysis, the axis references have been rotated to be fastened with $u^{out}_{AC,1}$. In this way, the actual DAB first harmonic voltages assume the form of (12) and (13)

$$\vec{u^{in}_{AC,1}} = |u^{out}_{AC,1}| + j\omega L_s |i^{out}_d| \tag{12}$$

$$|u^{out}_{AC,1}| = \frac{4}{\pi} u^{in}_{DC}\ k \sin\left(D_2 \frac{\pi}{2}\right) \tag{13}$$

where D_2 needs to be optimized for harmonic content minimization.

B. Harmonic Content Minimization

Minimizing the harmonic content of the output voltage allows for maximizing the energy associated to the first harmonic component. For achieving this goal, the optimal duty cycle D_2 can be simply evaluated imposing (3) equal to zero. In this way, the constraint for harmonic minimization is obtained as shown in (14)

$$\sin\left(nD_2 \frac{\pi}{2}\right) = 0 \implies nD_2 \frac{\pi}{2} = \pi \implies D_2 = \frac{2}{n} \tag{14}$$

in which the fundamental component is excluded regarding (1), and for which D_2 is imposed just equal to 1.

The optimal duty cycle has been found among the conditions in which $n = 1, 3, 5, 7, 9, 11, 13$, and the respective voltage square wave harmonic content are reported in Fig. 5. As can be seen, all the harmonics of the relative order are completely eliminated for the corresponding D_2 value. In Fig. 6, the Total Harmonic Distortion (THD) analysis concerning each scenario is reported, where the THD has been evaluated by (15)

$$THD(\%) = \frac{\sqrt{\sum_{n=3}^{+\infty}(u_{AC,n}^{out})^2}}{u_{AC,1}^{out}} 100. \tag{15}$$

The results highlight that the minimum THD condition is achieved for $n = 3$ i.e. $D_2 = 2/3$, which represents the best condition for the output voltage harmonic content minimization. Moreover, it can be noted that, after $n = 3$, the THD increases while the first harmonic module decreases, both monotonically with the harmonic order. This is due to the duty cycle that shrinks the square-wave voltage until it get to zero. This justify interrupting further scenario analysis, since it can be stated that there are no other optimum for higher n-values.

IV. Simulation Study

In order to evaluate the proposed TPS performances for controlling an All Electric Aircraft 270V DC-DC power conditioning system, a co-simulation study has been carried out concerning the DAB model and the control strategy developed on Plecs and Matlab-Simulink, respectively. The DAB model consider the parameters of a real laboratory converter prototype, which main characteristics are reported in Table I. In the proposed case study, the DAB converter controlled with TPS has 270V both in input and output ($k = 1$) for

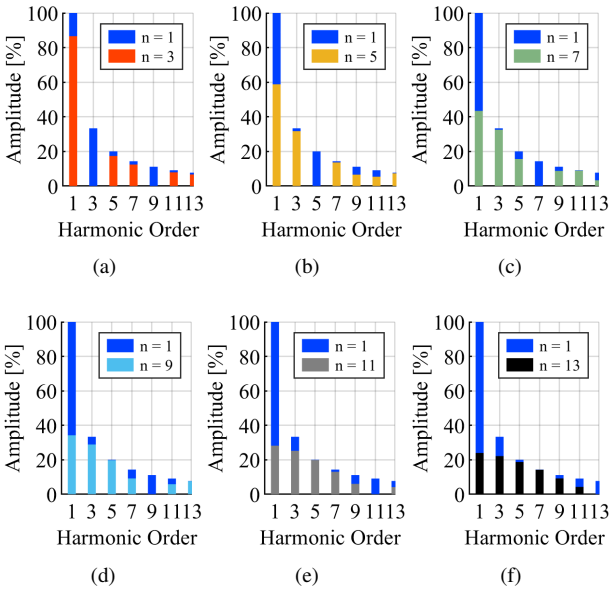

Fig. 5: Output voltage square wave harmonic content for $D_2 = 1$ and: a) $D_2 = \frac{2}{3}$; b) $D_2 = \frac{2}{5}$; c) $D_2 = \frac{2}{7}$; d) $D_2 = \frac{2}{9}$; e) $D_2 = \frac{2}{11}$; f) $D_2 = \frac{2}{13}$.

TABLE I: DAB Model Parameters

Maximum DC-Link Voltage	800	V
Switching Frequency	20	kHz
Maximum Continuous RMS Current	24	A
Rated Power	15	kVA
SiC MOSFET On Resistance	128	$m\Omega$
DC-Link Capacitor Banks	520	μF
Leakage Inductance	97	μH
Leakage Inductance Resistance	220	$m\Omega$
HFT Turn Ratio	1 : 1	–
HFT Magnetising Inductance	1.9	mH
HFT Winding Resistances	350	$m\Omega$

feeding the aircraft loads, for which a control strategy has been implemented for keeping the output voltage at the desired level when the load changes.

A. Control Strategy

The proposed control strategy block diagram is reported in Fig. 7. In particular, the PI controller defines the DAB output current i_d^{out}, from which the duty cycles D_1, D_2 and the phase-shift D_0 are evaluated resorting to (16), that in turn has been obtained resorting to (12), (13) and (14)

$$\begin{cases} D_0 = \frac{1}{\pi} \arctan\left[\frac{\omega L_s i_q^{out}}{u_{AC,1}^{out}}\right] \\ D_1 = \frac{2}{\pi} \arcsin\left[\frac{\sqrt{(u_{AC,1}^{out})^2 + (\omega L_s i_d^{out})^2}}{\frac{4}{\pi} u_{DC}^{in}}\right] \\ D_2 = 2/3. \end{cases} \tag{16}$$

The maximum power achievable with the proposed TPS control strategy can be evaluated when D_1 is equal to 1. In this condition, the maximum achievable D_0 is equal to 0.167 concerning (16). Considering that D_2 is fixed, the actual maximum active power is about 2.1kW, while the maximum rated appearent power is 2.4kVA, both evaluated concerning (10) and (11). As expected, the power of the converter is lower than the rated one reported in Table I of about 1/6 due to the actual behaviour of the TPS control strategy, which will be deepened in the next section.

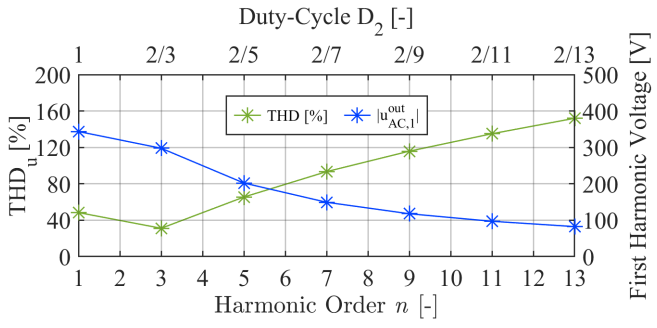

Fig. 6: Total Harmonic Distortion (THD) and Output Voltage First Harmonic Module Concerning both the Harmonic Order n and Duty Cycle D_2.

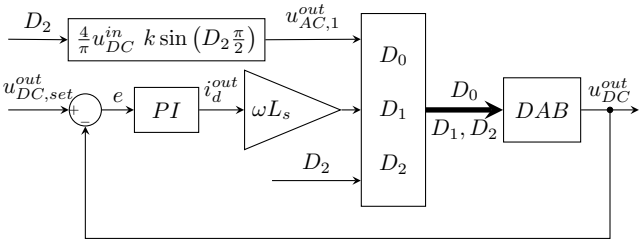

Fig. 7: Block diagram of the TPS voltage control system of the DAB.

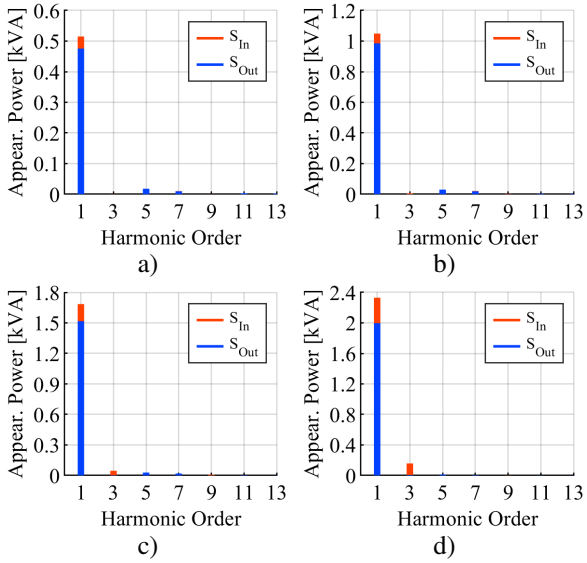

Fig. 8: Input and output apparent power of the first 13 harmonic component for a load value of a) 0.5kW; b) 1.0kW; c) 1.5kW; d) 1.95kW.

B. Simulation Results

The simulation study has been carried out for several output power conditions. In particular, 0.5kW, 1kW, 1.5kW and 1.95kW of AEA power load are considered. The squared voltage waveforms and its first-harmonic component for each output power conditions are shown in Fig. 10. Moreover, in Fig. 8, the apparent output power concerning the first thirteen harmonic components of both output voltage and current are shown. As expected, the transformer current have the same phase of the output voltage, as highlighted by the grey-dotted lines in Fig. 10. This aspect is confirmed in Fig. 8, where is shown that the output apparent power S_{out} corresponds to the active power required by the loads i.e. no reactive power is exchanged through the output side.

Moreover, Fig. 8 highlights that the first harmonic component power maximization goal is achieved, since no other components exchange a remarkable amount of power. In fact, Fig. 9 highlights a very low THD value achieved for the current, as an effect of the harmonic content reduction in the output voltage, with a minimum at 1.5kW output power. The maximization of the first harmonic component is also

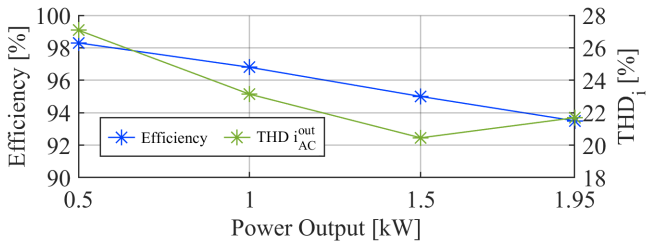

Fig. 9: DAB Efficiency and magnetic tank output current THD analysis in relation to the load value.

noticeable from Fig. 10, in which the peak value of both the current waveform and first harmonic component are very similar to each others. Furthermore, in Fig. 9 the converter efficiency concerning the conductive power losses is shown. It highlights that there is no particular effect related to the current wave THD. Moreover, as expected, its value decrease as the power output increase, with a maximum of about 98% and a minimum of 94% concerning the minimum and maximum output power, respectively.

In Fig. 11, the DC-link output and the capacitor bank currents are reported, which confirm the achievement of the zero-flow-back current goal for each output power. Moreover, it can be noted that extended intervals at zero-current are present. These are for ensuring the zero-flow-back current in the output side. As a consequence, a lower average current i.e. output power is present in the converter due to the TPS control strategy as foregrounded in the power analysis of Section IV-A.

In this way, the effectiveness of the proposed TPS control strategy is fully demonstrated, particularly in maximizing the power associated to the first harmonic component and eliminating the flow-back current contribution in the output DC-link.

Finally, in Fig. 12a and Fig. 12b the dynamic behaviour of both the output DC-link voltage and the control variables under step-load variations from 0.5kW to 1.5kW and *vice versa* are reported, showing a good dynamic performance.

V. Conclusion

In this paper, a co-simulation study of a laboratory-based-prototype Dual-Active Bridge converter is proposed. The modelling has been developed concerning the Fourier expansion of the magnetic thank voltage waveforms, particularly regarding the First Component Analysis. Moreover, a Triple Phase Shift that both minimize the voltage harmonic component and the DC-link flow-back current on the output side is proposed. The simulation results for an All Electric Aircraft 2.1kW, 270V DC/DC conversion stage is shown. The results demonstrates the achievement of the proposed target with an high conversion efficiency. In particular, the output power associated with the first harmonic component is maximized, while the reactive power contribution is removed. Finally, good control performances are achieved also for deep step-load variations.

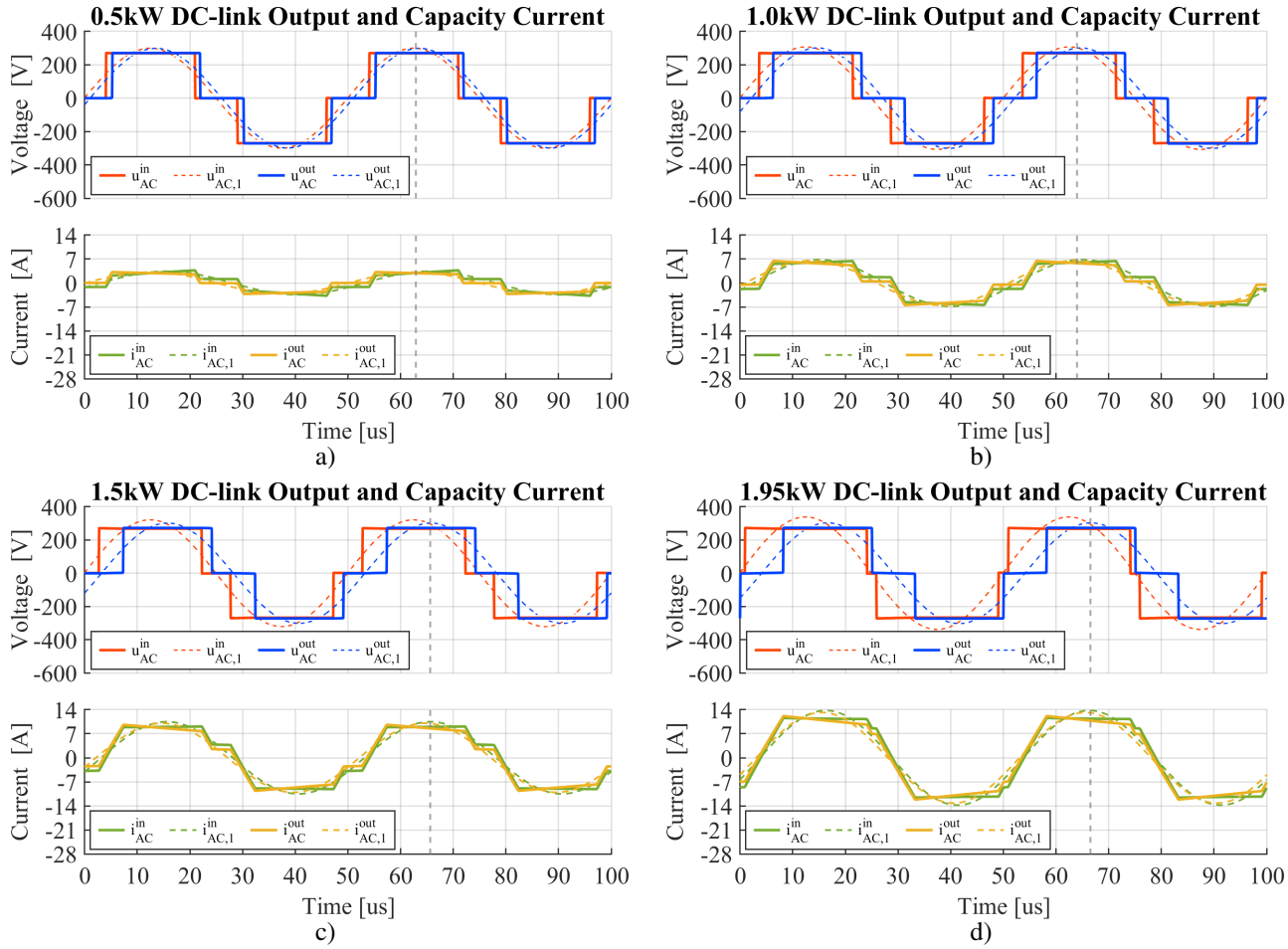

Fig. 10: DAB magnetic tank voltage and current waveforms for a load value of a) 0.5kW; b) 1.0kW; c) 1.5kW; d) 1.95kW.

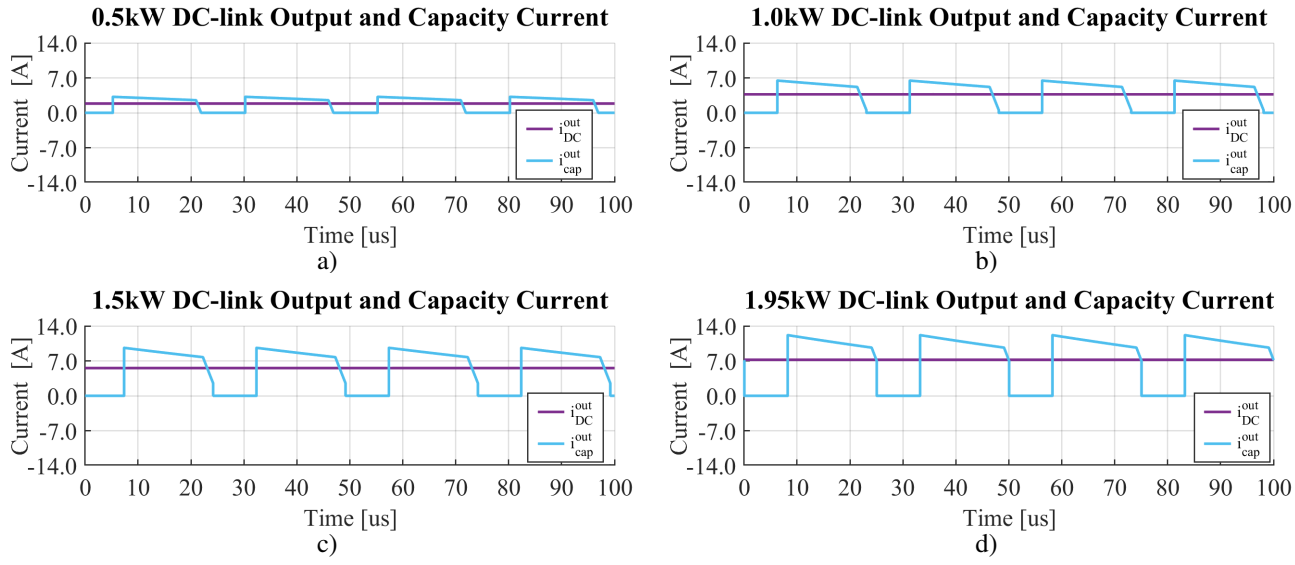

Fig. 11: DAB DC-link output and capacity current for a load value of a) 0.5kW; b) 1.0kW; c) 1.5kW; d) 1.95kW.

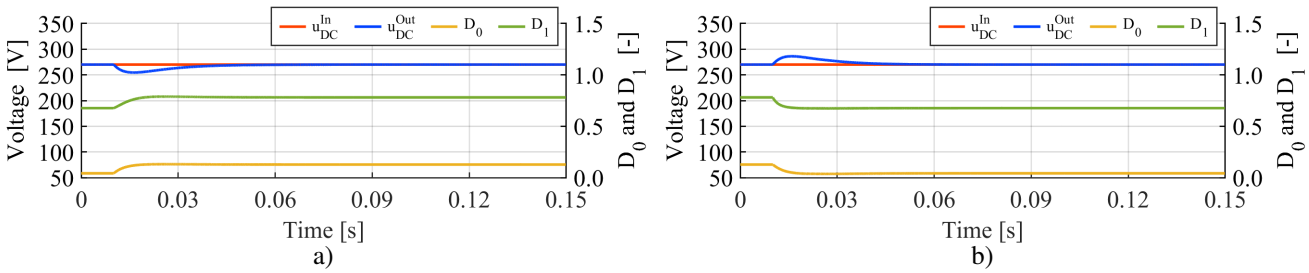

Fig. 12: DAB control response under step-load variations: a) from 0.5kW to 1.5kW; b) from 0.5kW to 1.5kW.

ACKNOWLEDGMENT

This work has been developed within the framework of the project e.INS- Ecosystem of Innovation for Next Generation Sardinia (cod. ECS 00000038) funded by the Italian Ministry for Research and Education (MUR) under the National Recovery and Resilience Plan (NRRP) - MISSION 4 COMPONENT 2, "From research to business" INVESTMENT 1.5, "Creation and strengthening of Ecosystems of innovation" and construction of "Territorial R&D Leaders".

REFERENCES

[1] A. Barzkar and M. Ghassemi, "Electric Power Systems in More and All Electric Aircraft: A Review," *IEEE Access*, vol. 8, pp. 169 314–169 332, 2020.

[2] G. Bossi, C. Buccella, C. Cecati, A. Damiano, A. Floris, and F. Simonetti, "A Converter Topology for Auxiliary Power System of an All Electric Aircraft," in *2023 IEEE Energy Conversion Congress and Exposition (ECCE)*, Oct. 2023, pp. 1605–1612.

[3] G. Bossi, M. Boi, N. Campagna, R. Miceli, and A. Damiano, "Evaluation of Triple Active Bridge for Power System of an All-Electric Aircraft." in *2023 International Conference on Clean Electrical Power (ICCEP)*, Jun. 2023, pp. 161–166.

[4] V. Karthikeyan, S. Rajasekar, S. Pragaspathy, and F. Blaabjerg, "Core Loss Estimation of Magnetic Links in DAB Converter Operated in High-Frequency Non-Sinusoidal Flux Waveforms," in *2018 IEEE International Conference on Power Electronics, Drives and Energy Systems (PEDES)*, Dec. 2018, pp. 1–5.

[5] S. Shao, M. Jiang, W. Ye, Y. Li, J. Zhang, and K. Sheng, "Optimal Phase-Shift Control to Minimize Reactive Power for a Dual Active Bridge DC–DC Converter," *IEEE Transactions on Power Electronics*, vol. 34, no. 10, pp. 10 193–10 205, Oct. 2019, conference Name: IEEE Transactions on Power Electronics.

[6] S. Luo, F. Wu, and G. Wang, "Improved TPS control for DAB DC–DC converter to eliminate dual-side flow back currents," *IET Power Electronics*, vol. 13, no. 1, pp. 32–39, 2020.

[7] G. Jean-Pierre, N. Altin, A. El Shafei, and A. Nasiri, "Efficiency Optimization of Dual Active Bridge DC– DC Converter with Triple Phase-Shift Control," in *2020 IEEE Energy Conversion Congress and Exposition (ECCE)*, Oct. 2020, pp. 1217–1222.

[8] N. Noroozi, A. Poorfakhraei, O. Zayed, A. Elezab, N. Keshmiri, M. Narimani, and A. Emadi, "RMS Current Minimization in a SiC-Based Dual Active Bridge Converter Using Triple-Phase-Shift Modulation," *IEEE Transactions on Industrial Electronics*, vol. 70, no. 7, pp. 7173–7182, Jul. 2023.

[9] N. Hou and Y. W. Li, "Overview and Comparison of Modulation and Control Strategies for a Nonresonant Single-Phase Dual-Active-Bridge DC–DC Converter," *IEEE Transactions on Power Electronics*, vol. 35, no. 3, pp. 3148–3172, Mar. 2020.

[10] C. Song, A. Sangwongwanich, Y. Yang, Y. Pan, and F. Blaabjerg, "Analysis and Optimal Modulation for 2/3-Level DAB Converters to Minimize Current Stress With Five-Level Control," *IEEE Transactions on Power Electronics*, vol. 38, no. 4, pp. 4596–4612, Apr. 2023.

[11] C. Song, A. Sangwongwanich, Y. Yang, and F. Blaabjerg, "Optimal Control of Multi-Level DAB Converters for Soft-Switching and Minimum Current Stress," *IEEE Transactions on Power Electronics*, pp. 1–14, 2024.

[12] F. An, W. Song, K. Yang, S. Yang, and L. Ma, "A Simple Power Estimation With Triple Phase-Shift Control for the Output Parallel DAB DC–DC Converters in Power Electronic Traction Transformer for Railway Locomotive Application," *IEEE Transactions on Transportation Electrification*, vol. 5, no. 1, pp. 299–310, Mar. 2019.

[13] D. Das and K. Basu, "Optimal Design of a Dual-Active-Bridge DC–DC Converter," *IEEE Transactions on Industrial Electronics*, vol. 68, no. 12, pp. 12 034–12 045, Dec. 2021.

[14] G. Jean-Pierre, N. Altin, A. El Shafei, and A. Nasiri, "Overall Efficiency Improvement of a Dual Active Bridge Converter Based on Triple Phase-Shift Control," *Energies*, vol. 15, no. 19, p. 6933, Sep. 2022.

[15] B. Zhao, Q. Song, W. Liu, G. Liu, and Y. Zhao, "Universal High-Frequency-Link Characterization and Practical Fundamental-Optimal Strategy for Dual-Active-Bridge DC-DC Converter Under PWM Plus Phase-Shift Control," *IEEE Transactions on Power Electronics*, vol. 30, no. 12, pp. 6488–6494, Dec. 2015.

[16] D. Mou, L. Yuan, Q. Luo, Y. Li, C. Liu, J. Zheng, and Z. Zhao, "Overview of Multi-Degree-of-Freedom Modulation Techniques for Dual Active Bridge Converter," *IEEE Journal of Emerging and Selected Topics in Power Electronics*, vol. 11, no. 6, pp. 5724–5737, Dec. 2023.

[17] H. Naseem and J.-K. Seok, "Reactive Power Controller for Single Phase Dual Active Bridge DC–DC Converters," *IEEE Access*, vol. 11, pp. 141 537–141 546, 2023.

[18] S. S. Shah and S. Bhattacharya, "A Simple Unified Model for Generic Operation of Dual Active Bridge Converter," *IEEE Transactions on Industrial Electronics*, vol. 66, no. 5, pp. 3486–3495, May 2019.

[19] J. Huang, Y. Wang, Z. Li, and W. Lei, "Unified Triple-Phase-Shift Control to Minimize Current Stress and Achieve Full Soft-Switching of Isolated Bidirectional DC–DC Converter," *IEEE Transactions on Industrial Electronics*, vol. 63, no. 7, pp. 4169–4179, Jul. 2016.